Residue Gly[1326] of the N-type Calcium Channel α[1B] Subunit Controls Reversibility of ω-Conotoxin GVIA and MVIIA Block*

Zhong-Ping Feng‡§¶‖, Jawed Hamid‡¶, Clinton Doering‡§, Gregory M. Bosey**,
Terrance P. Snutch**‡‡, and Gerald W. Zamponi‡§§

From the ‡Departments of Physiology & Biophysics and Pharmacology & Therapeutics, Neuroscience Research Group,
University of Calgary, Calgary, Alberta T2N 4N1, Canada, §NeuroMed Technologies Inc., Vancouver V6T 1Z4, Canada,
and the **Biotechnology Laboratory, University of British Columbia, Vancouver V6T 1Z3, Canada

We recently reported that amino acid residues contained within a putative EF hand motif in the domain III S5-H5 region of the α[1B] subunit affected the relative barium:calcium permeability of N-type calcium channels (Feng, Z. P., Hamid, J., Doering, C., Jarvis, S. E., Bosey, G. M., Bourinet, E., Snutch, T. P., and Zamponi, G. W. (2001) J. Biol. Chem. 276, 5726–5730). Since this region partially overlaps with residues previously implicated in block of the channel by ω-conotoxin GVIA, we assessed the effects of mutations in the putative EF hand domain on channel block by ω-conotoxin GVIA and the structurally related ω-conotoxin MVIIA. Both of the toxins irreversibly block the activity of wild type α[1B] N-type channels. We find that in addition to previously identified amino acid residues, residues in positions 1326 and 1332 are important determinants of ω-conotoxin GVIA blockade. Substitution of residue Glu[1332] to arginine slows the time course of development of block. Point mutations in position Gly[1326] to either arginine, glutamic acid, or proline dramatically decrease the time constant for development of the block. Additionally, in the G1326P mutant channel activity was almost completely recovered following washout. A qualitatively similar result was obtained with ω-conotoxin MVIIA, suggesting that common molecular determinants underlie block by these two toxins. Taken together the data suggest that residue Gly[1326] may form a barrier, which controls the access of peptide toxins to their blocking site within the outer vestibule of the channel pore and also stabilizes the toxin-channel interaction.

It is well established that peptide toxins isolated from marine snails have the propensity to potently and highly selec-

tively inhibit the activities of a number of different types of voltage- and ligand-gated ion channels (1–5). These toxins include blockers of skeletal muscle sodium channels (μ-conotoxin (6–8)), the nicotinic acetylcholine receptor (α-conotoxins (9, 10)), and blockers of voltage-dependent calcium channels (ω-conotoxins (2)). Among the family of ω-conotoxins, two prominent members are ω-conotoxin GVIA, a 27-amino acid peptide derived from the Conus geographus sea snail, and ω-conotoxin MVIIA, a 25-amino acid toxin isolated from the venom of the Conus magus marine snail (2). Both of these toxins potently block N-type calcium channels from a variety of species and nerve tissues (11–14). Block develops rapidly and is only incompletely reversible even after prolonged washout (12). Both toxins have been reported to display a high degree of selectivity for the N-type calcium channel α[1B] subunit (15), and ω-conotoxin GVIA has become a commonly used tool for the identification of native N-type calcium currents.

While little is presently known concerning the toxin structural requirements, which underlie the high affinity and selectivity of ω-conotoxins GVIA and MVIIA for N-type calcium channels, some of the N-type calcium channel regions that participate in the blocking interaction have been elucidated. Utilizing a chimeric channel approach in combination with site-directed mutagenesis, Ellinor and co-workers (16) identified crucial components of the binding site of ω-conotoxin GIVA in the external vestibule of the α[1B] channel in the domain III S5-S6 region, suggesting that this toxin likely acts via physical occlusion of the pore. While the binding site for ω-conotoxin MVIIA has not yet been identified via molecular biological techniques, both biochemical and electrophysiological data suggest that ω-conotoxin MVIIA competes with ω-conotoxin GVIA for a subgroup, or at least partially overlapping, receptor site (2, 17).

We have recently reported that point mutations in an external EF hand homology motif located on the N-type calcium channel α[1B] subunit immediately adjacent to the ω-conotoxin GVIA binding site identified by Ellinor et al. (16) affects the permeation characteristics of the channel (18). In view of its proximity to the putative ω-conotoxin GVIA receptor site, we investigated whether mutations in this region could affect the characteristics of ω-conotoxin GVIA and MVIIA block of the channel. We report here that certain point mutations within the putative EF hand motif increase the affinity of the channel for ω-conotoxin GVIA. Moreover, one of the mutations, a replacement of residue Gly[1326] with proline, is sufficient to dramatically enhance the unblocking rate of the toxin such that block by both ω-conotoxin GVIA and MVIIA is fully reversible over a time course of <10 min. Hence, residues immediately outside the region identified previously by Ellinor et al. (16) contribute to block of N-type calcium channels by ω-conotoxins,
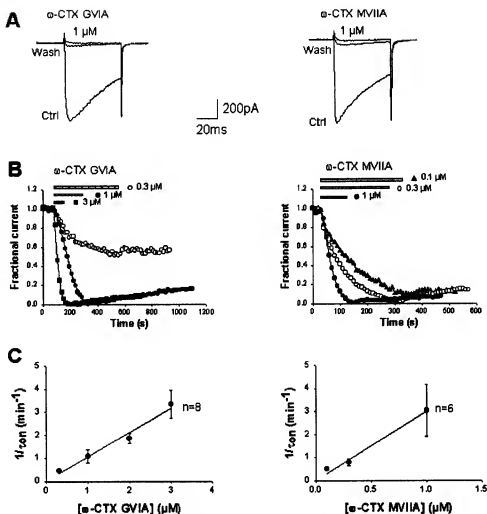
EXHIBIT B: PAGE 1 OF 8

FIG. 1. **Block of transiently expressed N-type (α_{1B}+β_{1b}+α_2-δ) calcium channels by ω-conotoxins (*CTX*) GVIA and MVIIA.** *A*, current records illustrating the effects of the two toxins. Block is complete and virtually irreversible in response to washout for 10 min. Currents were elicited by stepping from a holding potential of -100 mV to a test potential of $+20$ mV. *B*, representative time courses of development of block and of recovery from block by ω-conotoxin GVIA and ω-conotoxin MVIIA. In both cases, the block develops more rapidly at higher toxin concentrations. Note that block by ω-conotoxin MVIIA develops more rapidly than that of ω-conotoxin GVIA. *C*, dependence of the inverse of the time constant for development of block, τ, on the toxin concentration, *[CTX]*. The *solid lines* are linear regressions (fitted with the equation: $1/\tau = k_{on}*[\text{conotoxin}] + k_{off}$), whose slopes reflect the blocking rate constants (k_{on}) and whose intercepts on the *y* axis are equivalent to the unblocking rate constants (k_{off}). The rate constants obtained from the fits are as follows: ω-conotoxin GVIA, $k_{on} = 1.06$ μM^{-1} min^{-1}, $k_{off} = 0.011$ min^{-1}; ω-conotoxin MVIIA, $k_{on} = 2.93$ μM^{-1} min^{-1}, $k_{off} = 0.07$ min^{-1}. *Error bars* denote S.E. values.

FIG. 2. *A*, amino acid sequence of the α_{1B} domain III S5-H5 region. The putative EF hand calcium binding domain (□) spans residues Glu^{1321} to Glu^{1332}. Amino acid residues implicated previously in ω-conotoxin GVIA block (16) (O) are located between Gln^{1327} and Gln^{1339}. *B*, proposed membrane topology of the N-type calcium channel α_1 subunit (20) indicating the location of the putative EF hand motif. The *inset* illustrates the possible locations of the key residues relative to the pore forming p-loop structure of the channel as proposed by Ellinor *et al.* (16).
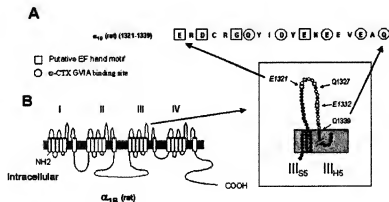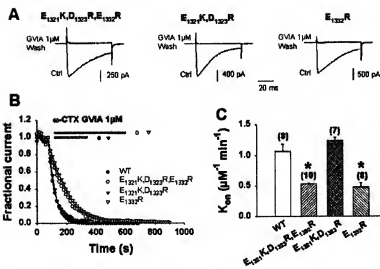
FIG. 3. **Effect of mutations in positions 1321, 1323, and 1332 on toxin block.** *A*, current records obtained with mutant (E1321K,D1323R, E1332R), (E1321K,D1323R), or E1332R channels (coexpressed with β_{1b} and α_2-δ) in the absence and presence of 1 μM ω-conotoxin GVIA. Note that all three mutants are irreversibly and completely blocked at this toxin concentration. *B*, representative time course of development of block of wild type and mutant N-type calcium channels by 1 μM ω-conotoxin GVIA. Note that the triple mutant and the single E1332R mutant channel display slowed blocking kinetics compared with the wild type or the (E1321K,D1323R) mutant construct. *C*, blocking rate constants obtained with the wild type and mutant channels. The K_{on} values were obtained by fitting linear regressions as shown in Fig. 1*C* for each individual experiment. *Error bars* denote S.E. values, *numbers in parentheses* reflect numbers of experiments, and the *asterisks* indicate statistical significance relative to the wild type channels ($p < 0.05$).

and a single amino acid residue in this region is sufficient to control the reversibility of toxin block.

EXPERIMENTAL PROCEDURES

Site-directed Mutagenesis—The G1326P, E1332R, D1323R, and E1321R point mutation constructs have been described by Feng *et al.* (18). The R1325D, G1326K, G1326E, and G1326Y constructs were generated as described by Feng *et al.* (18). In brief, a *SplI-AflII* fragment (~4.5 kilobases) was excised from the full-length cytomegalovirus-α_{1B} (CMV) construct and ligated into pSL1180. Site-directed mutagenesis was carried out using the QuikChange mutagenesis kit (Stratagene) and successful mutagenesis was confirmed via DNA sequencing. Subsequently, the mutated *SplI-AflII* fragment was introduced into the full-length clone in the cytomegalovirus (CMV) expression vector via restriction enzyme digestion and ligation and its presence confirmed by restriction endonuclease digestion and DNA sequencing.

Tissue Culture and Transient Transfection—Human embryonic kidney tsa-201 cells were maintained in a 37 °C CO$_2$ incubator in standard Dulbecco's modified Eagle's medium (supplemented with 10% fetal bovine serum, 200 units/ml penicillin, and 0.2 mg/ml streptomycin). The cells were split at 85% confluence using trypsin EDTA and plated on glass coverslips at 5–10% confluence. The cells were then allowed to recover for ~12 h at 37 °C before transfection. Immediately before transfection, the medium was replaced, and the cells were transiently transfected with cDNAs encoding for calcium channel α_{1B}, β_{1b}, and α_2-δ subunits and EGFP (at a molar ratio of 1:1:1:0.3) via the calcium phosphate method. After 12 h, the cells were washed with fresh medium, allowed to recover for additional 12 h, and subsequently stored at 28 °C in 5% CO$_2$ for 1–3 days before whole cell recording. Recordings were performed using an Axopatch 200B amplifier (Axon Instruments, Foster City, CA) linked to a personal computer equipped with pClamp version 7.0. Patch pipettes (Sutter borosilicate glass, BF 150-86-15) were pulled using a Sutter P-87 microelectrode puller and subsequently fire-polished using a Narashige microforge.

Whole Cell Patch Clamp Recordings and Data Analysis—The whole cell patch clamp recordings (membrane ruptured) procedures used here were similar to those described by Beedle and Zamponi (19). Briefly, cells were transferred to a 3-cm culture dish containing recording solution comprised of 20 mM BaCl$_2$ (or CaCl$_2$), 1 mM MgCl$_2$, 10 mM HEPES, 40 mM TEA[1]-Cl, 10 mM glucose, 87.5 mM CsCl (pH 7.2 with

[1] The abbreviation used is: TEA, tetraethylammonium.

TEA-OH). Pipettes with resistances of 2–4 MΩ were filled with internal recording solution containing 108 mM cesium methanesulfonate, 4 mM MgCl$_2$, 9 mM EGTA, 9 mM HEPES (pH 7.2 with TEA-OH). After patch rupture, cell capacitance was neutralized, and series resistance was compensated. Currents were elicited by stepping from a holding potential of −100 mV to various test potentials using Clampex 7.0 software and an Axopatch 200 B amplifier (Axon Instruments, Foster City, CA). ω-Conotoxin GVIA (RBI Chemicals) and MVIIA (Sigma) were dissolved first, respectively, in water and acetic acid and then diluted in the external recording solution. Solutions containing various concentrations of toxin were delivered directly to the cells by means of a gravity-driven microperfusion system, which allows complete solution exchanges in less than 1 s. Currents underwent little if any rundown during the time course of a typical experiment. Data were filtered at 1 kHz and digitized at a sampling frequency of 2 kHz. Data were analyzed using Clampfit (Axon Instruments). All curve fittings were carried out using Sigmaplot 4.0 (Jandel Scientific). The time constant, τ, for onset of block was determined from the equation $I(t)/I(t = 0) = \exp(-t/\tau)$, where $I(t)$ is the current amplitude at time t after application of the toxin, and $I(t = 0)$ is the control current amplitude immediately prior to toxin application. Statistical analysis was carried out using SigmaStat 2.0 (Jandel Scientific). Differences between mean values from each experimental group were tested using a Student's t test for two groups and one way analysis of variance for multiple comparisons. Differences were considered significant if $p < 0.05$. All error bars given reflect S.E values, numbers in parentheses indicate number of cells.

RESULTS

ω-Conotoxins GVIA and MVIIA Irreversibly Block N-type Calcium Channels—Fig. 1 illustrates the effects of ω-conotoxin GVIA and MVIIA on N-type (α_{1B}+β_{1b}+α_2-δ) calcium channels transiently expressed in HEK tsa-201 cells. The application of 1 μM of either toxin completely removes current activity, which cannot be recovered following washout over the time course of 10 min. Fig. 1*B* compares the time courses of N-type channel block for various concentrations of both toxin. For both toxins the time course of development of block is accelerated with increasing toxin concentration, although on average development of ω-conotoxin MVIIA block occurs about three times more rapidly than that of ω-conotoxin GVIA. Similar to what has been previously reported for both native channels (14) and α_{1B} channels transiently expressed in *Xenopus* oocytes (16),
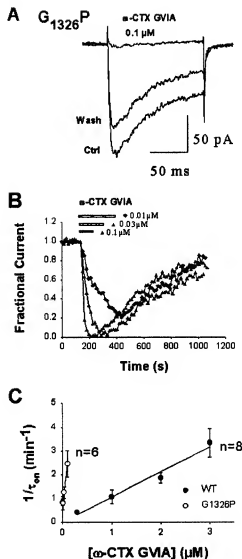
FIG. 4. *ω-Conotoxin (CTX) GVIA block of the G1326P mutant.* *A*, current records illustrating block of the G1326P ($+\beta_{1b}+\alpha_2\text{-}\delta$) construct by 100 nM ω-conotoxin GVIA. Note that the effects of the toxin are almost completely reversed following washout. *B*, representative time course of development of, and recovery from, block of the G1326P mutant by different concentrations of ω-conotoxin GVIA. Note the reversibility of toxin block. *C*, kinetic analysis of block of wild type and G1326P mutant channels by ω-conotoxin GVIA. The data for the wild type channel are the same as in Fig. 1. Note the dramatic increase in the slope of the regression line and the larger *y* intercept obtained with the mutant channel. The blocking and unblocking rate constants for the G1326P mutant obtained from the fit were, respectively, 17.5 μM^{-1} min^{-1} and 0.72 min^{-1}. *Error bars* denote S.E. values.

block of both toxins was only poorly reversible such that even prolonged washout (7–15 min) resulted in the recovery of only a minor fraction of the N-type current. Fig. 1*C* illustrates the dependence of the inverse of the time constant for development of block on the toxin concentration. Consistent with a bimolecular interaction between the toxin molecule and the channel, the relation was well described by a linear fit in the case of each of the two toxins. The blocking rate constants (k_{on}), obtained from the regression lines, were, respectively, 1.06 and 2.93 μM^{-1} min^{-1} for ω-conotoxins GVIA/MVIIA, consistent with the data shown in Fig. 1*B*. However, it is not possible to accurately determine the unblocking rate constants (k_{off}) from either the

regression lines or from the time course of recovery from block because of the poor reversibility of the blocking action.

Mutations in the Domain III S5-H5 Region Affect ω-Conotoxin GVIA Block—We have previously reported that high voltage-activated calcium channels contain a highly conserved putative EF hand motif within the domain III S5-H5 region (18). As shown in Fig. 2 for the α_{1B} subunit, this region is localized immediately adjacent to a series of amino acid residues, which have been implicated in ω-conotoxin GVIA block of the channel (16). In a previous study we showed that replacement of the three negative charges in the putative EF hand motif with positively charged residues, or substitution of the central glycine (Gly^{1326}), resulted in an ablation of the differential selectivity of the channel between barium and calcium ions without affecting other major biophysical properties of the channel such as activation, inactivation, or block by cadmium ions (18). To test whether this region of the channel might modulate the blocking action of ω-conotoxin GVIA, we first expressed the triple (E1321K,D1323R,E1332R) α_{1B} mutant in HEK tsa-201 cells (together with the ancillary β_{1b} and $\alpha_2\text{-}\delta$ subunits) and examined the dose dependence of ω-conotoxin GVIA blocking kinetics of the mutant channel. As shown in Fig. 3, the time course of development of ω-conotoxin GVIA block in the triple mutant channel was significantly slowed compared with that observed with the wild type channel, indicating that one or a combination of the three substituted residues contribute to ω-conotoxin GVIA block of the channel. Nonetheless, the application of 1 μM concentrations of the toxin was sufficient to eliminate all current activity, and as with the wild type channel, block of the mutant channel was irreversible (Fig. 3, *A* and *B*). To determine which of the three residues was responsible for mediating the slowing of the blocking kinetics, we examined ω-conotoxin GVIA block of both a single E1332R and a double (E1321K,D1323R) mutant. As seen in Fig. 3*B*, a single substitution of residue 1332 with arginine was sufficient to account for the slowing of the blocking kinetics, whereas the double mutant behaved similar to the wild type channel. This is shown quantitatively in form of a comparison of the blocking rate constants of ω-conotoxin GVIA block of the wild type and the mutant channels (Fig. 3*C*). Mutation in position Glu^{1332} to arginine resulted in a 2-fold reduction in k_{on} and suggests that the glutamate contributes in a significant manner to ω-conotoxin GVIA block of N-type calcium channels.

In our previous study examining permeation, we replaced the central glycine residue (Gly^{1326}) within the putative external EF hand domain with proline (18). To determine whether this substitution affects block of the channel by ω-conotoxin GVIA, the G1326P mutant was expressed with the appropriate ancillary subunits in tsa-210 cells, and ω-conotoxin GVIA blocking kinetics were examined. Fig. 4 shows that development of block was accelerated 30-fold compared with the wild type channel (Fig. 4*B*). More strikingly, upon washout of the toxin current activity could be almost completely recovered over the time course of about 10 min (Fig. 4, *A* and *B*). Since the time course for development of block is inversely proportional to the sum of blocking and unblocking rates, such an increase in the rate of recovery from block is predicted to contribute to the observed 30-fold decrease in the time constant for development of block. To isolate any direct effects of the mutation on the true blocking rate constant, the time course for development of block was determined at several toxin concentrations, and the inverse of the time constant of development of block was plotted as a function of toxin concentration. As shown in Fig. 4*C*, the relation is nicely described by a linear fit. Furthermore, from the slope and the *y* intercept of the regression line, both the blocking (k_{on} = 17.51 μM^{-1} min^{-1}) and the
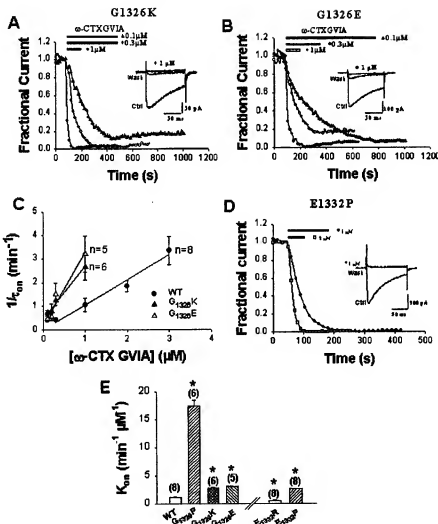
FIG. 5. *A* and *B*, effects of different substitutions for Gly^{1326} on ω-conotoxin (CTX) GVIA block in the form of representative time courses. Note that unlike in case of G1326P, block of G1326K and G1326E channels remains irreversible. *C*, kinetic analysis of toxin block as described in Fig. 1C. Note that the blocking rate constant is increased in both mutants compared with wild type channels. The blocking and unblocking rate constants obtained from the fits were as follows: G1326K, k_{on} = 2.18 μM^{-1} min^{-1}, k_{off} = 0.5 min^{-1}; G1326E, k_{on} = 3.06 μM^{-1} min^{-1}, k_{off} = 0.21 min^{-1}). *D*, effect of a substitution of Glu^{1332} to proline. Unlike the G1326P mutant, the E1332P mutant cannot be recovered from toxin block. *E*, comparison of the blocking rate constants obtained with wild type and mutant channels. The blocking rate constants were obtained as described in the legend to Fig. 3C. *Error bars* denote S.E. values, *numbers in parentheses* are numbers of experiments, and *asterisks* denote statistical significance relative to control. All mutants shown in the figure were coexpressed with β_{1b} and α_2-δ subunits.

unblocking (k_{off} = 0.72 min^{-1}) rate constants were found to be significantly increased in the G1326P mutant compared with the wild type channel, indicating that the access of the toxin to its binding site is enhanced in the mutant, but concomitantly the stability of the binding interaction is dramatically reduced.

To determine whether this effect is also observed with other substitutions at the G1326 position, we generated three additional mutations (G1326K, G1326E, and G1326Y). Interestingly, the G1326Y mutant resulted in channels that could no longer be functionally expressed. However, the G1326K and G1326E mutants expressed well, and as shown in Fig. 5A and B, the time course of development of block with these channels remained irreversible over the time course of a typical experiment. This is also evident from the kinetic analysis presented in Fig. 5, C and E, where the slope of the regression line (and hence, the blocking rate constant) is clearly increased, whereas the intercept on the *ordinate* is similar to that obtained with the wild type channels. To test whether the presence of a proline residue *per se* was sufficient to render the channels reversible from ω-conotoxin GVIA block, we generated an E1332P mutant. As shown in Fig. 5D, ω-conotoxin GVIA block of this mutant was not reversible, because the presence of a proline *per se* near in the putative EF hand motif is insufficient to render the channels reversible from toxin block. Interestingly, the effect of the

E1332P mutation on the blocking rate constant was opposite to that obtained with the E1332R construct, which tended to slow the blocking kinetics.

Overall, our data indicate that at least two additional residues besides those identified previously by Ellinor *et al.* (16) are important determinants of ω-conotoxin GVIA block and that residue 1326 is an important factor in controlling both access of the toxin and the strength of interaction with the channel.

The G1326P Mutant Results in Reversible ω-Conotoxin MVIIA Binding—The striking effects observed with the G1326P mutant raise an obvious question: is ω-conotoxin MVIIA block affected in a similar manner? As shown in Fig. 6, both the development and the reversibility of block of the channel by ω-conotoxin MVIIA are dramatically enhanced in the Gly^{1326} mutant. However, there were subtle differences in the manner by which the mutation affected block by the two toxins. Whereas the effects of the mutation on recovery from ω-conotoxin MVIIA block was even more pronounced than those observed with the GVIA isoform (*i.e.* complete recovery from block after 5 min), the effect of the mutation on the blocking rate constant was greater for ω-conotoxin GVIA (16-fold increase in k_{on}) than for ω-conotoxin MVIIA (7-fold increase). Nonetheless, these data indicate that there is significant overlap in the channel structural determinants of the access of ω-conotoxins GVIA and MVIIA to their binding sites,
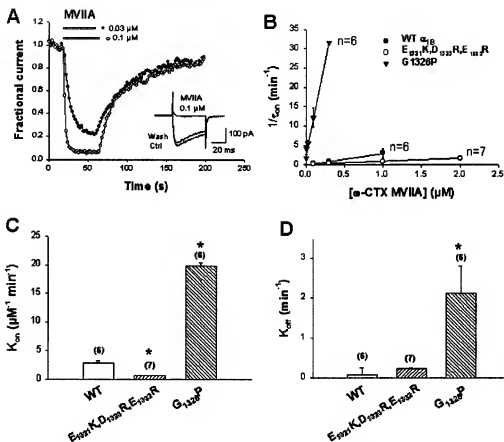
FIG. 6. **Effect of mutations in positions 1326 and 1332 on ω-conotoxin (CTX) MVIIA block.** *A,* representative time course of development of block and recovery from block for the G1326P mutant. Note the rapid reversibility of blocking action. *B,* kinetic analysis of ω-conotoxin MVIIA block of wild type α_{1B} or mutant (E1321K,D1323R,E1332R), and G1326P mutant channels (coexpressed with β_{1a} and α_2-δ). The blocking and unblocking rate constants obtained from the fits were as follows: G1326P, k_{on} = 19.87 μM^{-1} min^{-1}, k_{off} = 2.11 min^{-1}; triple mutant, k_{on} = 0.68 μM^{-1} min^{-1}, k_{off} = 0.23 min^{-1}. *C* and *D,* blocking and unblocking rate constants obtained with wild type, G1326P and (E1321K,D1323R,E1332R) channels. Data were obtained via linear regressions as shown in Fig. 1C for each individual experiment. The *error bars* denote S.E. valuess, *numbers in parentheses* reflect the numbers of individual experiments, and *asterisks* denote significance relative to wild type channels.

FIG. 7. **Possible model accounting for the effects of the G1326P mutation on the time course of development and recovery from ω-conotoxin (CTX) block.** In the wild type channel, residue Gly[1326] may form a barrier that restricts egress of the toxin to its blocking site but also prevents the dissociation of the toxin once docked to the receptor. The introduction of the proline residue may remove this barrier, thus providing more ready access and concomitantly, a less stable binding interaction.

Wild type channel   **G1326P channel**

ω-CTX

G1326 P

Intracellular
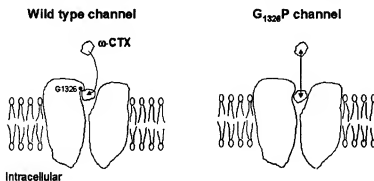
consistent with biochemical data showing that both toxins compete for a common binding site (11).

DISCUSSION

Peptide toxins isolated from venomous animal species are among the most potent inhibitors of voltage-gated calcium channels (2, 21). Calcium channel blocking peptides appear to fall into two major classes: gating blockers, which allosterically inhibit channel opening (*e.g.* ω-agatoxin IVA (22, 23) and ω-grammotoxin-S1A (24–26)), and pore blockers, which physically prevent ion permeation (*e.g.* ω-conotoxins GVIA (16) and

MVIIC (11, 17) and ω-agatoxin III (27, 28)). To date, the exact sites of action of the gating inhibitors on the calcium channel α_1 subunit remain enigmatic. Furthermore, unlike in the case of potassium channels (5, 29) and sodium channels (7, 30–32), the detailed molecular mechanisms by which calcium channels are inhibited by pore-blocking toxins remain poorly understood. To date, there has only been one comprehensive study that has examined the channel structural determinants of ω-conotoxin GVIA block. Using a series of chimeras between α_{1A} P/Q-type and α_{1B} N-type calcium channels, Ellinor *et al.* (16) were able to show that the domain III S5-S6 region was critically important

for block of N-type calcium channels by ω-conotoxin GVIA. In particular, residues Gln[1327], Glu[1334], Glu[1337], and Gln[1339] were found to contribute to ω-conotoxin GVIA block, with Glu[1337] mediating the largest effect. In the present study, we have identified two additional residues that appear to be important for the interaction of the toxin with pore-blocking toxins, residues Gly[1326] and Glu[1332]. Since these residues are conserved in α_{1A} and α_{1B} channels (33), their contributions to toxin block could not have been detected with a chimeric approach. It is interesting to note that amino acid substitutions adjacent to the region identified by Ellinor *et al.* (16) (*i.e.* Glu[1332] and Gly[1326]) mediated a more pronounced effect on ω-conotoxin GVIA block, compared with mutations that occur further upstream (*i.e.* Gln[1321] and Asp[1322]). This could perhaps suggest that residue 1326 might form an outer boundary for the ω-conotoxin GVIA receptor site. This is further supported by data obtained with an R1325E construct, which did not display altered toxin block (not shown).

We have previously reported that the expression of the G1326P, E1332R, and a double (E1321K,D1323N) mutant resulted in currents that no longer supported a differential permeability to calcium and barium ions, but otherwise displayed biophysical properties that did not differ significantly from those of the wild type channels, including activation, inactivation, and block by divalent cations (18). We attributed the effects on ion selectivity to a highly localized specific disruption of the function of a putative calcium binding EF hand spanned by residues 1321–1332, rather than a global structural rearrangement of the α_{1B} subunit. The observation that substitutions in positions 1321 and 1323 did not affect ω-conotoxin GVIA block is consistent with a highly localized and specific effect of amino acid substitutions in these positions on ion selectivity. Moreover, that substitutions in positions Gly[1326] and Glu[1332] did not affect channel gating, and cadmium block (18) is also consistent with a localized effect of these mutations on the toxin-channel interaction.

The most pronounced effect on toxin action was observed with the G1326P construct in that the blocking rate constant was increased 16-fold, and block became entirely reversible. This suggests that the mutation increases both the accessibility of the binding site and at the same time results in a less stable interaction between the toxin and the channel. Interestingly, other substitutions in this position, while increasing the rate of development of block did not affect the reversibility of block. It is well established that proline residues act as helix breakers and thus may mediate a more pronounced effect on the local structure of the channel. However, the presence of a proline in this region of the channel *per se* is not sufficient to render toxin block reversible, since the E1332P construct did not affect recovery from toxin block. The dramatic effects on the reversibility of block seen with the G1326P mutant cannot be explained by a simple change in toxin affinity, since this mutation resulted in only a ~4-fold increase in the equilibrium dissociation constants of the two toxins as determined from the ratio of unblocking and blocking time constants. Instead, we envision a scenario in which residue Gly[1326] restricts the access of the toxin to its docking site (Fig. 7). Once the toxin has docked to its receptor site, the barrier formed by Gly[1326] would aid in the stabilization of the channel toxin interaction. Upon mutation of Gly[1326] to proline, this barrier may be removed, thereby providing greater access to the blocking site, but concomitantly resulting in a less stable interaction. Substitutions of Gly[1326] with other types of amino acid residues may not be as effective in removing the putative access barrier and, hence, affect the time constant for development of block and unblock to a smaller degree.

It is more difficult to speculate about the basis for the effects of substitutions in position Glu[1332]. It is possible that this residue forms a low affinity contact point between the toxin and the channel. Alternatively, changes in this residue may allosterically affect the interaction of the toxin with residue Glu[1334], which was previously identified as an important determinant of ω-conotoxin GVIA block (16). The change in the time constant of development of block observed with the E1332R and E1332P constructs are unlikely due to a change in net charge of the channel, since neither the double (E1321K,D1323R) nor the R1325E substitution significantly affected toxin block.

A major finding is that mutations that affect block of the channel by ω-conotoxin GVIA also affect the action of ω-conotoxin MVIIA. To date, the only evidence suggesting an overlap between the blocking sites for the two toxins had come from competitive binding studies (2). Here, we have demonstrated for the first time at the amino acid level that the two toxins share some of the same channel molecular determinants. The two toxins share a similar disulfide dose arrangement comprised of six conserved cysteine residues, but only about 27% in sequence identity among their non-cysteine residues (2, 34). This suggests that one or more of the conserved toxin residues may interact with residue 1326 on the calcium channel or that the three-dimensional folding of the toxin backbone is a key determinant for blocking action. The latter scenario would fit with the model shown in Fig. 7, which predicts that toxins with an overall similarity in their backbone structure would be similarly affected by the presence/absence of an access barrier. Regardless of the underlying mechanism, our data show that a single amino acid residue in the domain III S5-H5 region is sufficient to control access of two structurally distinct peptides from two different cone snail species, suggesting that the basic mechanism by which these two toxins block channel activity is highly conserved.

In summary, our data identify two residues (Gly[1326] and Glu[1332]) in the α_{1B} subunit, which are important determinants of ω-conotoxin block. The G1326P mutant may serve as a convenient tool for further investigation into the detailed mechanisms underlying ω-conotoxin block of N-type calcium channels by allowing direct access to the effects of any additional mutations on the channel or the toxin molecule on both blocking and unblocking kinetics. In view of the clinical use of ω-conotoxin MVIIA as an analgesic (35, 36), such information may aid in the design of more effective calcium channel therapeutics.

REFERENCES

1. Quik, M. (1992) *Mol. Neurobiol.* **6**, 19–40
2. Olivera, B. M., Miljanich, G. P., Ramachandran, J., and Adams, M. E. (1994) *Annu. Rev. Biochem.* **63**, 823–867
3. Favreau, P., Le Gall, F., Benoit, E., and Molgo, J. (1999) *Acta Physiol. Pharmacol. Ther. Latinoam.* **49**, 257–267
4. Passani, L. D., Becerril, B., Delepierre, M., and Tytgat, J. (1999) *Eur. J. Biochem.* **264**, 287–300
5. Tenenholz, T. C., Klenk, K. C., Matteson, D. R., Blaustein, M. P., and Weber, D. J. (2000) *Rev. Physiol. Biochem. Pharmacol.* **140**, 135–185
6. Mocydlowski, E., Olivera, B. M., Gray, W. R., and Strichartz, G. R. (1986) *Proc. Natl. Acad. Sci. U. S. A.* **83**, 5321–5325
7. Becker, S., Prusak-Sochaczewski, E., Zamponi, G., Beck-Sickinger, A. G., Gordon, R. D., and French, R. J. (1992) *Biochemistry* **31**, 8229–8238
8. French, R. J., Prusak-Sochaczewski, E., Zamponi, G. W., Becker, S., Kularatna, A. S., and Horn, R. (1996) *Neuron* **16**, 407–413
9. Kulak, J. M., Nguyen, T. A., Olivera, B. M., and McIntosh, J. M. (1997) *J. Neurosci.* **17**, 5263–5270
10. Luo, S., Kulak, J. M., Cartier, G. E., Jacobsen, R. B., Yoshikami, D., Olivera, B. M., and McIntosh, J. M. (1998) *J. Neurosci.* **18**, 8571–8579
11. Woppmann, A., Ramachandran, J., and Miljanich, G. P. (1994) *Mol. Cell. Neurosci.* **5**, 350–357
12. Fox, J. A. (1995) *Pflugers Arch.* **429**, 873–875
13. Boland, L. M., and Bean, B. P. (1993) *J. Neurosci.* **13**, 516–533
14. Boland, L. M., Morrill, J. A., and Bean, B. P. (1994) *J. Neurosci.* **14**, 5011–5027
15. Williams, M. E., Brust, P. F., Feldman, D. H., Patthi, S., Simerson, S., Maroufi, A., McCue, A. F., Velicelebi, G., Ellis, S. B., and Harpold, M. M. (1992) *Science* **257**, 389–395
16. Ellinor, P. T., Zhang, J. F., Horne, W. A., and Tsien, R. W. (1994) *Nature* **372**, 272–275

17. McDonough, S. I., Swartz, K. J., Mintz, I. M., Boland, L. M., and Bean, B. P. (1996) *J. Neurosci.* 15, 2612–2623
18. Feng, Z. P., Hamid, J., Doering, C., Jarvis, S. E., Bosey, G. M., Bourinet, E., Snutch, T. P., and Zamponi, G. W. (2001) *J. Biol. Chem.* 276, 5726–5730
19. Beedle, A. M., and Zamponi, G. W. (2000) *Biophys. J.* 79, 260–270
20. Catterall, W. A. (2000) *Annu. Rev. Cell Dev. Biol.* 16, 521–555
21. Adams, M. E., Myers, R. A., Imperial, J. S., and Olivera, B. M. (1993) *Biochemistry* 30, 12566–12570
22. Mintz, I. M., Venema, V. J., Swiderek, K. M., Lee, T. D., Bean, B. P., and Adams, M. E. (1992) *Nature* 27, 827–829
23. McDonough, S. I., Mintz, I. M., and Bean, B. P. (1997) *Biophys. J.* 72, 2117–2128
24. Lampe, R. A., Defeo, P. A., Davison, M. D., Young, J., Herman, J. L., Spreen, R. C., Horn, M. B., Mangano, T. J., and Keith, R. A. (1993) *Mol. Pharmacol.* 44, 451–460
25. Piser, T. M., Lampe, R. A., Keith, R. A., and Thayer, S. A. (1995) *Mol. Pharmacol.* 48, 131–139
26. McDonough, S. I., Lampe, R. A., Keith, R. A., and Bean, B. P. (1997) *Mol. Pharmacol.* 52, 1095–1104
27. Ertel, E. A., Warren, V. A., Adams, M. E., Griffin, P. R., Cohen, C. J., and Smith, M. M. (1994) *Biochemistry* 33, 5098–5108
28. Mintz, I. M. (1994) *J. Neurosci.* 14, 2844–2853
29. Miller, C. (1995) *Neuron* 15, 5–10
30. Chahine, M., Sirois, J., Marcotte, P., Chen, L., and Kallen, R. G. (1998) *Biophys. J.* 75, 236–246
31. Li, R. A., Tsushima, R. G., Kallen, R. G., and Backx, P. H. (1997) *Biophys. J.* 73, 1874–1884
32. Li, R. A., Ennis, I. L., Velez, P., Tomaselli, G. F., and Marban, E. (2000) *J. Biol. Chem.* 275, 27551–27558
33. Stea, A., Soong, T. W., and Snutch, T. P. (1995) in *Handbook of Receptors and Channels: Ligand- and Voltage-gated Ion Channels* (North, R. A., ed) pp. 113–141, CRC Press Inc., Boca Raton, FL
34. Olivera, B. M., Gray, W. R., Zeikus, R., McIntosh, J. M., Varga, J., Rivier, J., de Santos, V., and Cruz, L. J. (1985) *Science* 230, 1338–1343
35. Ridgeway, B., Wallace, M., and Gerayli, A. (2000) *Pain* 85, 287–289
36. Penn, R. D., and Paice, J. A. (2000) *Pain* 85, 291–296

EXHIBIT B: PAGE 8 OF 8